

P1.6 WINTER STORM FORECASTING AS A TWO-STEP PROCESS:
THE 26-27 NOVEMBER 2001 SNOWSTORM

Martin A. Baxter* Sam Ng Charles E. Graves
James T. Moore

Saint Louis University
Earth and Atmospheric Sciences
St. Louis, MO

1. INTRODUCTION

In order to forecast snowfall amounts for a winter extratropical cyclone (ETC), the forecaster must engage in a two-step process. First, current dynamic and thermodynamic fields must be analyzed in conjunction with numerical model forecasts to determine a quantitative precipitation forecast (QPF). This QPF represents the liquid equivalent expected to precipitate from the system. To convert this liquid equivalent to a snowfall amount, a snow to liquid equivalent ratio must be determined. The 26-27 November snowfall event contained heavy banded snowfall, suggesting unique kinematic and dynamic processes were instrumental in the organization of the precipitation. The goal of this paper is to examine interactions between the synoptic and mesoscale within heavy banded snowfall, as well as interactions between the microscale and mesoscale in the form of snow to liquid equivalent ratios.

First, a conceptual model of the processes that lead to heavy banded snowfall will be described. Secondly, a case study will be examined to demonstrate the viability of the conceptual model. Finally, the observed snow to liquid equivalent ratios will be analyzed with the aim of identifying the processes that determine them.

2. CONCEPTUAL MODEL OF COLD-SEASON MESOSCALE PROCESSES CONTRIBUTING TO BANDED HEAVY SNOWFALL

Combining a review of the literature with the authors' own research, three processes significantly contribute to the development of heavy banded snowfall associated with ETC's: the development of a trough of warm air aloft (trowal), mid-level fron-

togenesis, and the reduction of equivalent potential vorticity (EPV).

a. THE TROWAL STRUCTURE

The trowal was originally postulated by Canadian meteorologists in the 1940's and 1950's as a line connecting the crests of the thermal wave at successive heights (Crocker et al. 1947, Godson 1951). Martin (1998a) reintroduced the trowal concept as the three-dimensional sloping intersection of the upper cold-frontal portion of the warm occlusion with the warm-frontal zone. In a cross section, it can be viewed as a sloping canyon of moist, high θ_e air. The diagnosis of the trowal is crucial as the sensible weather correlates more with the trowal rather than the surface warm occlusion.

To understand the origins of the trowal, it is necessary to consider the positions of the cold conveyor belt (CCB) and warm conveyor belt (WCB) which are part of the system-relative airflow through the ETC. As defined by Carlson (1980), the WCB represents the poleward slantwise ascension of warm, moist air, turning anticyclonically as it approaches the troposphere and polar jet. The CCB originates north of the warm front, flowing westward relative to the low pressure center before turning anticyclonically and merging with the WCB in the upper troposphere. Schultz (2001) challenges this notion of the CCB, demonstrating that the CCB more likely follows a cyclonically-curved path as it reaches the westward side of the low. The WCB need not follow the same path for every system, but instead may turn cyclonically around the low center as the cyclone becomes occluded (Martin 1998b, 1999). The trowal is represented by the westernmost extension of the WCB.

*Corresponding author address: Martin A. Baxter, Earth and Atmos. Sciences, Saint Louis University, St. Louis MO 63103; email: baxterma@eas.slu.edu

b. FRONTOGENESIS

Frontogenesis is calculated in two-dimensional form as,

$$F = \frac{1}{2} |\nabla\theta| (Def_r \cos(2\beta) - Div) \quad (1)$$

which is the abbreviated version of the frontogenesis equation derived by Miller (1948). Here the resultant deformation (Def_r) and divergence (Div) act to increase the potential temperature gradient in the vicinity of a baroclinic zone. Mid-level frontogenesis is often generated in a deformation zone to the northwest of the trowal airstream due to the confluence of the WCB (trowal airstream) with the colder, drier, airstream to the north. A direct thermal circulation results from an increase in the gradient of potential temperature (frontogenesis) as the atmosphere attempts to restore thermal wind balance (Holton 1992). The upward motion resulting from this direct thermal circulation can enhance heavy banded snowfall.

c. REDUCTION OF EPV

EPV can be computed using the three-dimensional form derived by McCann (1995) which best lends itself to gridded datasets, i.e.,

$$EPV = g \left[\frac{\partial\theta_{es}}{\partial x} \frac{\partial v_g}{\partial p} - \frac{\partial\theta_{es}}{\partial y} \frac{\partial u_g}{\partial p} - \left(\frac{\partial v_g}{\partial x} - \frac{\partial u_g}{\partial y} + f \right) \frac{\partial\theta_{es}}{\partial p} \right] \quad (2)$$

where u_g and v_g are the x and y components of the geostrophic wind. EPV in a saturated environment is a function of horizontal and vertical gradients of θ_{es} and the thermal wind. When $EPV < 0$ (hence the term ‘‘reduction’’ of EPV) parcels will be unstable to either vertical or slantwise motions. The unstable zone is most likely to form to the southeast of an occluding low as the dry conveyor belt descends cyclonically into the ETC circulation overlaying moist air below (Nicosia and Grumm 1999). This low-mid level moist air is likely to result from the WCB (Schultz 2001). To the north of the conditionally unstable region a region of conditional symmetric instability (CSI) forms in which the atmosphere is stable with respect to horizontal and vertical displacements, but unstable with respect to slantwise motions.

Nicosia and Grumm (1999) noted that the mid-level frontogenesis increases the geostrophic wind shear which in turn increases the differential moisture advection. Thus EPV reduction results from those processes associated with mid-level frontogenesis and the system relative flow through the ETC.

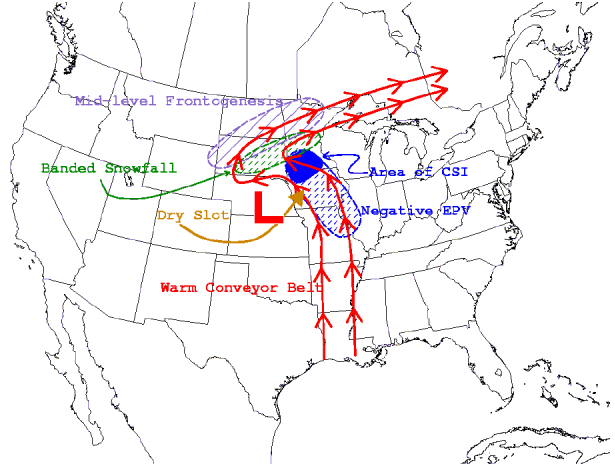


Figure 1: Conceptual model of those processes contributing to banded heavy snowfall in ETCs

The processes contributing to the development of the trowal and the mid-level frontogenesis are not a coincidence, rather they are the result of simultaneous events associated with the mature stage of cyclogenesis. The non-linearity of the positive feedbacks between the processes associated with the trowal, mid-level frontogenesis, and reduction of EPV necessitate a process-oriented approach toward heavy banded snowfall forecasting. The aforementioned three processes leading to banded heavy snowfall are schematically depicted in Fig. 1.

3. APPLICATION OF THE CONCEPTUAL MODEL TO THE 26-27 NOVEMBER 2001 SNOWSTORM

During the 60 h period ending 1200 28 November 2001, a major winter storm moved through the upper Midwest. The lowest central pressure associated with the ETC was 997.9 hPa on 0600 UTC 26 November 2001 when the system became occluded over the south-central plains. Although one typically diagnoses trowals with strong cyclones, it is possible to have significant (though more subtle) trowals develop with more modest cyclones depending on the system-relative flow (Smith 2003). This work will focus on the 0000 UTC 27 November 2001 time period, as at this time the surface low pressure was at the approximate midpoint of the track of heavy snowfall (Fig. 2).

The total snowfall accumulation associated with the ETC was in excess of 50.8 cm (20 in) in various locations including Nebraska, South Dakota, Minnesota, Wisconsin, and the Upper Peninsula of Michigan (Fig. 3). The snowband had an aver-

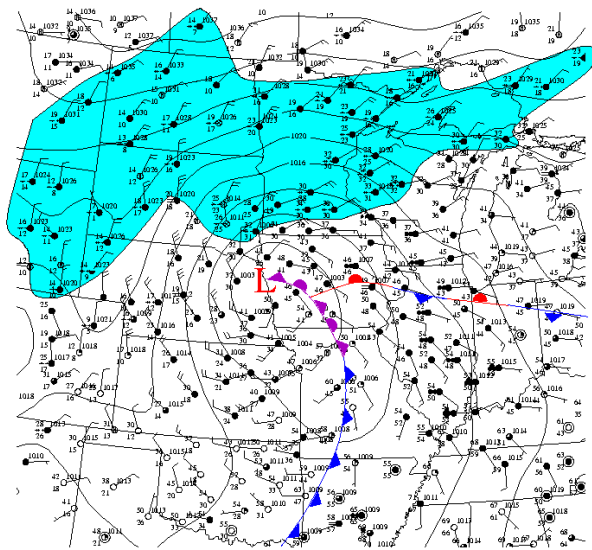


Figure 2: Surface map for 0000 UTC 27 November 2001. Cyan shading indicates region where snow was observed.

age half-width of approximately 97.6 km (60.7 mi), clearly indicative of mesoscale banding.

The trowal structure is evident in both plan and three-dimensional views. A trowal structure was diagnosed at 600 hPa at 0000 UTC 27 November as a cyclonically-oriented ridge of high θ_e extending to the northwest of the surface low (Fig. 4). The trowal structure can be viewed three-dimensionally as a sloping canyon of high θ_e air (Fig. 5). As isentropic surfaces slope downward toward warm air, it is clear that the trowal develops as the westernmost extension of the WCB. This sloping canyon of high θ_e air is transporting warm, moist air well to the northwest of the surface low pressure.

The precipitation resulting from the moist-adiabatic ascent of the trowal airstream is enhanced by the direct thermal circulation forced by the mid-level frontogenesis. The mid-level frontogenesis is generated as the trowal airstream becomes confluent with the colder, drier airstream to the north-northwest of the surface occlusion. To demonstrate this, 800-600 hPa frontogenesis was plotted along with system-relative streamlines on the 296 K isentropic surface at 0000 UTC 27 November 2001 (Fig. 6); the system velocity was computed to be 5.2 m s^{-1} at 190.8° over the last 12 h.

The maximum frontogenesis stretches over a west-east oriented axis from North Dakota to the Upper Peninsula of Michigan just north of the area of heaviest snowfall. From a three-dimensional perspective the region of frontogenesis slopes upward from low

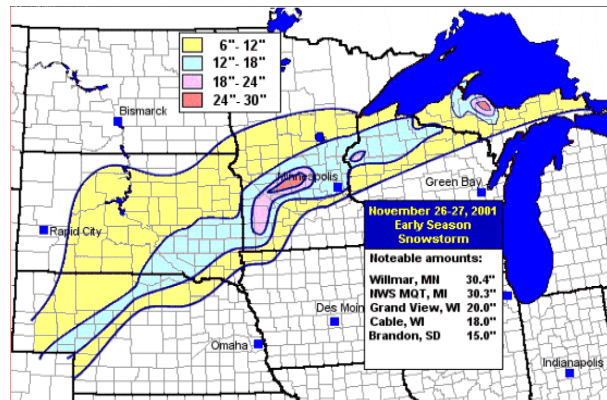


Figure 3: Snowfall totals for 26-27 November 2001 (courtesy NWSFO Milwaukee/Sullivan, Wisconsin).

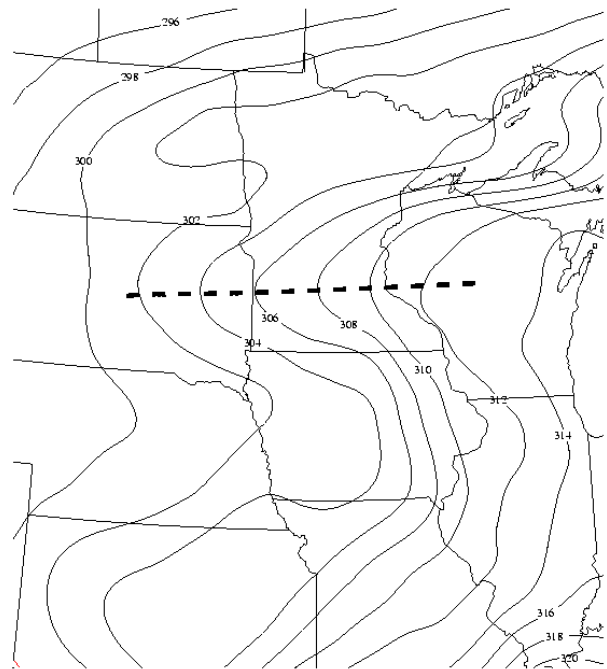


Figure 4: 600 hPa θ_e for 0000 UTC 27 November 2001 from RUC-II initialization. Dashed line indicates axis of trowal.

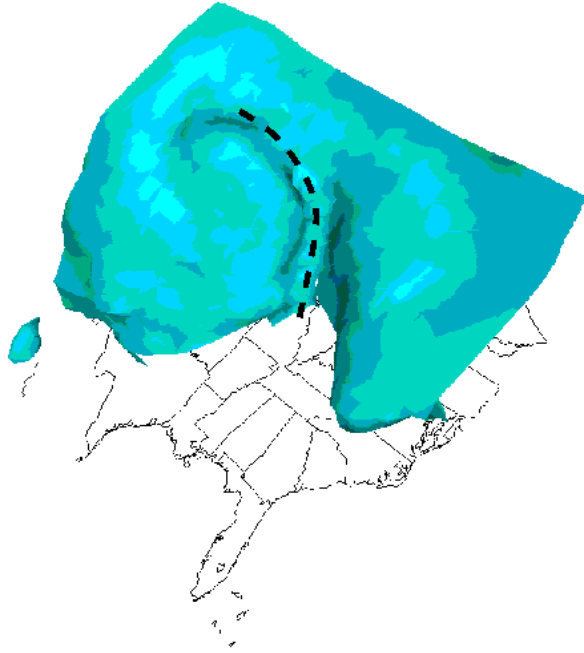


Figure 5: Three-dimensional view of the 306 K θ_e surface from the southeast on 0000 UTC 27 November 2001 from RUC-II initialization.

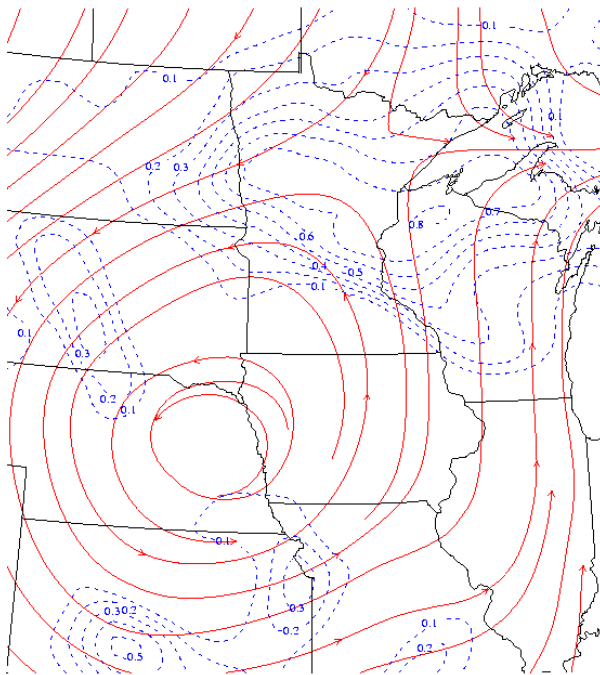


Figure 6: Average 800-600 hPa frontogenesis ($\text{K } 100 \text{ km}^{-1} \text{ 3 h}^{-1}$) and 296 K isentropic system-relative streamlines from RUC-II initialization for 0000 UTC 27 November 2001.

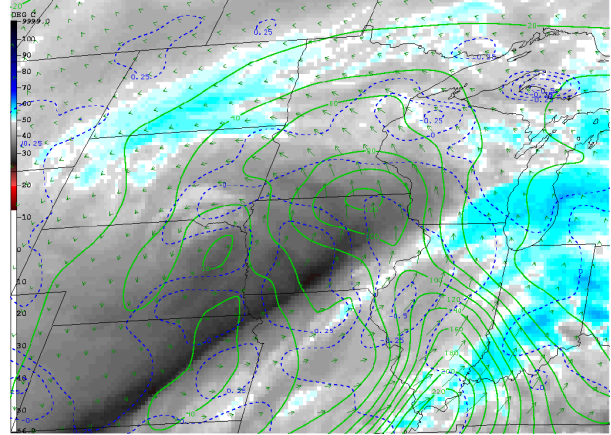


Figure 7: GOES 8 Water Vapor Imagery (darker areas indicate drier regions), 850 hPa moisture transport vectors ($\text{g kg}^{-1} \text{ m s}^{-1}$; in green), 600 hPa Saturated EPV in PVU ($10^{-6} \text{ m}^2 \text{ s}^{-1} \text{ K kg}^{-1}$; in blue), at 0000 UTC 27 November 2001 from RUC-II initialization.

levels under the trowal airstream to the northwest of the the trowal where it is seen in the middle levels ($\sim 600\text{-}700$ hPa) of the troposphere.

Lastly, an area of weak to negative EPV at 600 hPa is present in Illinois and Iowa to the south of the area of heavy snowfall (Fig. 7). In the lower levels, 850 hPa moisture transport vectors show the moist air streaming northward from the Gulf of Mexico. In the vertical, the area of weak to negative EPV lies between the low-level moisture transport and the middle tropospheric dry slot depicted in the water vapor image. This demonstrates that a region of weak to negative EPV is associated with convective instability. In this case the flow through the reduction of EPV region was predominantly over an area where surface temperatures were above freezing, hence the area of heavy banded snowfall was to the north of the maximum EPV reduction. Note that the heavy snow does not have to be in a region of negative EPV, since even weak symmetric stability can both contract and strengthen the region of upward motion over meso- β scales, thus contributing to heavy snowfall over a narrow band.

4. SNOW TO LIQUID EQUIVALENT RATIOS FOR THE 26-27 NOVEMBER 2001 SNOWSTORM

Snow to liquid equivalent ratios can vary considerably from the conventionally assumed 10 to 1, causing inaccurate snowfall depth forecasts even when the amount of liquid water created by the ETC is

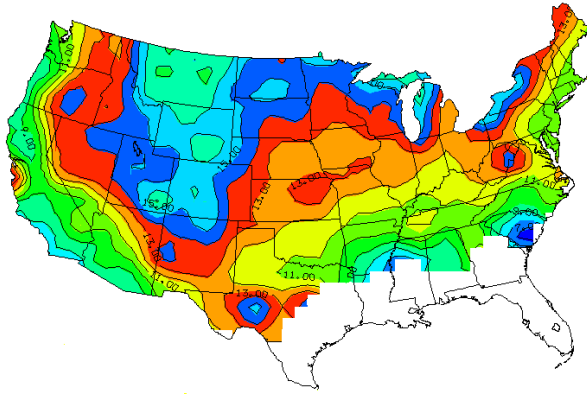


Figure 8: Average Snow to Liquid Ratios computed over 1971 to 2000 using National Weather Service Cooperative Observer Summary of the Day data.

correctly predicted. A 30-year (1971-2000) climatology of snow to liquid equivalent ratio has been computed for the United States using National Weather Service Cooperative Observer Summary of the Day data (Fig. 8).

According to this research, the average snow to liquid equivalent ratio value for much of the United States is closer to 13 to 1. The value of the snow to liquid equivalent ratio is determined by both in-cloud and sub-cloud microphysical interactions, some of which can be extracted through an examination of vertical profiles of temperature and moisture.

For the 26-27 November 2001 event, average snow to liquid equivalent ratios were computed over 40,000 km boxes (Fig. 9) for the 24 h period ending 1200 UTC 27 November 2001. While significant variability may be present within each box, measurement errors are substantial enough to cause difficulty in discriminating between the variation due to measurement error and actual variations in SLR, hence the need to examine snow to liquid equivalent ratio on a larger scale. Fig. 9 displays considerable stratification of the average snow to liquid equivalent ratios, with values of 8-12 to 1 in the southern and eastern portions of the snowfall and values of 16-20 in the northwestern portion. Snow to liquid equivalent ratios in this case were lower than the climatological values in the southern and eastern portions of the snowfall and higher than the climatological values in the northwestern portion of the snowfall.

As surface conditions are of great importance in diagnosing a snow to liquid equivalent ratio, a surface meteogram for the 24 h period ending 1200 UTC 27 November 2001 is presented (Fig. 10). All sta-

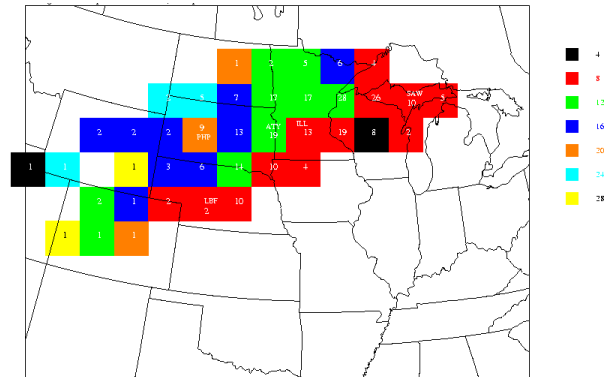


Figure 9: Average snow to liquid equivalent ratio over 40,000 km boxes for the 24 h period ending 12 UTC 27 November 2001. Numbers inside boxes represent number of observations included in the average. Stations shown are North Platte, NE (LBF), Phillip, SD (PHP), Watertown, SD (ATY), Wilmar, MN (ILL), and Gwinn, MI (SAW).

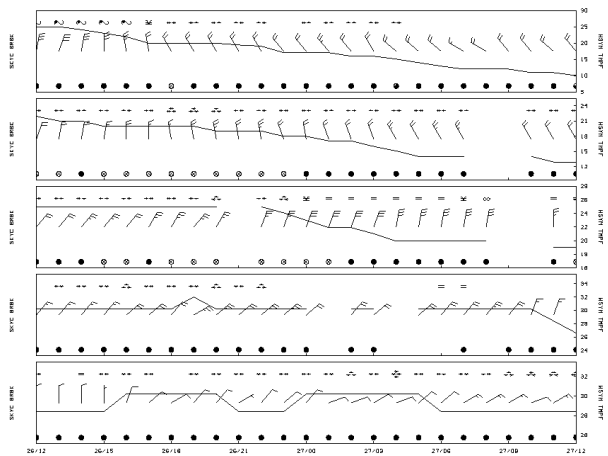


Figure 10: Surface meteogram displaying weather symbol, wind speed in knots, temperature in °F, and sky condition for the 24 h period ending 12 UTC November 2001. Stations shown (from top to bottom) are LBF, PHP, ATY, ILL, SAW.

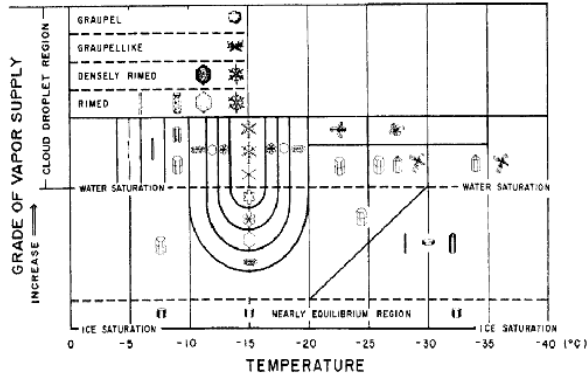


Figure 11: Natural crystal habit related to temperature and degree of supersaturation, Magono and Lee (1966).

tions exhibit strong winds (some in excess of 15.4 m s^{-1} (30 kts)), likely reducing the accuracy of the measurements. Of key importance in the surface time-series is the variation of temperature between stations. Surface temperatures at LBF, ILL, and SAW are all much closer to the freezing point than are temperatures at PHP and ATY. Snow to liquid equivalent ratios at LBF, ILL, and SAW ranged from 8-12 to 1, while snow to liquid equivalent ratios at PHP and ATY ranged from 16-24 to 1.

Three-hourly Eta model initializations were formatted for display in BUFKIT, with linearly interpolated values filling in the remaining hours to create an hourly sounding. Examining the vertical temperature and moisture profiles, one can attempt to determine the type of crystals that form and how they will change as they fall through the cloud and sub-cloud layers. The work of Magono and Lee (1966) demonstrates the observed crystal structure for a given temperature and moisture content (Fig. 11). The maximum growth rate is expected to occur near the level of maximum upward motion within the cloud, corresponding to the greatest water vapor delivery (Auer and White 1980). Waldstreicher (2001) shows that when maximum vertical motion is collocated with temperatures favorable for dendritic crystal growth (-12°C to -18°C), heavy snowfall can occur.

Examining the sounding for ILL (Fig. 13; the location of heaviest snowfall), temperatures in the layer from 650 to 500 hPa (the level of maximum vertical motion as shown in Fig. 12) average -15.8°C . According to Fig. 11, this configuration leads to crystals with a dendritic habit. As the crystals fall, they encounter a moist layer extending to the

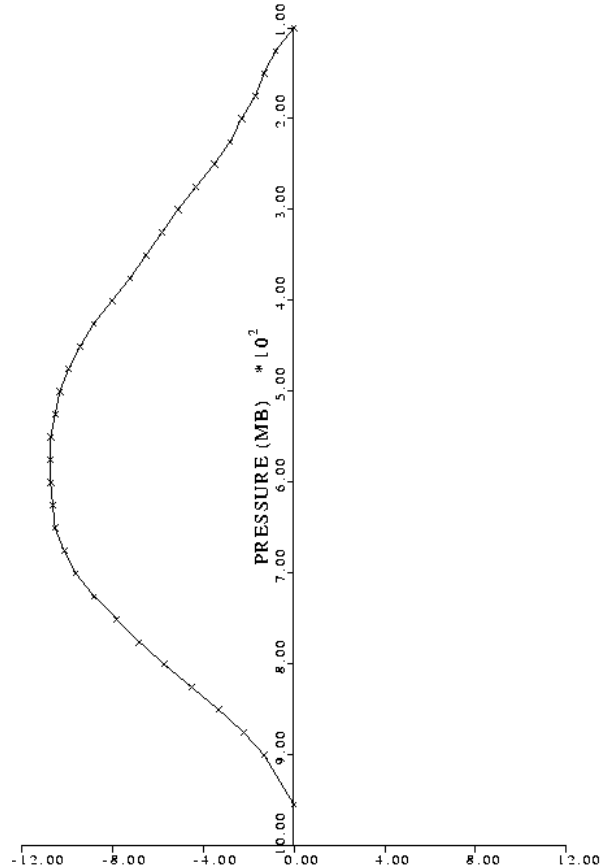


Figure 12: Omega ($\mu\text{bars s}^{-1}$) using the Bellamy triangle method (Bellamy 1949) with stations Rapid City, SD (RAP), International Falls, MN (INL), and Chanhassen, MN (MPX).

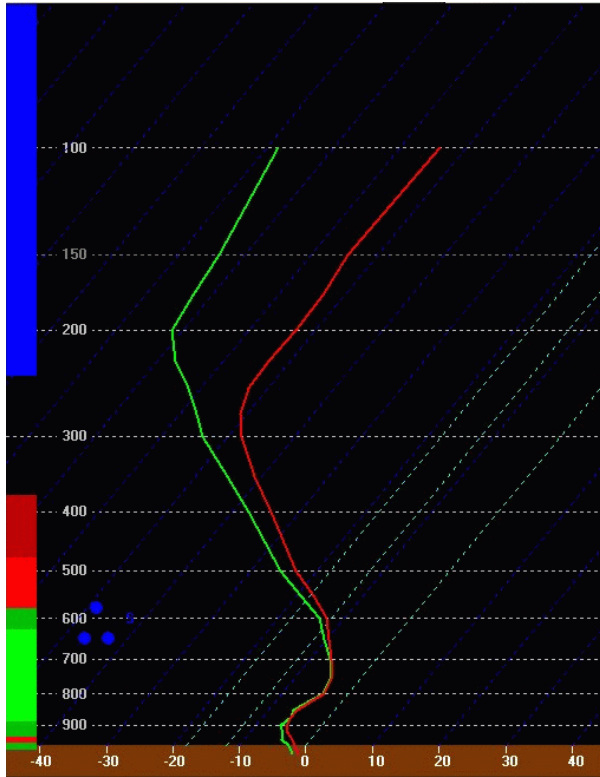


Figure 13: BUFKIT Skew-T for ILL at 0000 UTC 27 November 2001. Temperatures and dewpoints are in $^{\circ}\text{C}$, with relative humidity plotted on the left hand side of the figure (blue $< 30\%$, black 30 - 70%, red 70 - 90%, dark green 90 - 95%, light green $> 95\%$).

surface with relative humidities greater than 90%. Temperatures increase through the layer down to a 1000 hPa temperature of -0.3°C . The warming through the moist layer implies riming of the crystals. When rimed crystals fall to the surface, they become densely packed, creating a relatively low snow to liquid ratio.

Examining the sounding for PHP (Fig. 14), temperatures in the 650 to 500 hPa level average -19.5°C , very near the dendritic formation range. Examining a slightly lower level of 700 to 550 gives a more favorable average temperature of -16.9°C . As the crystals fall, temperatures warm to only -5.4°C , while relative humidities never exceed 90%. This implies that less riming occurred at PHP than ILL, therefore the crystals at PHP retain more of their original habit. The dendrite habit contains more air space in the interstices of the crystal, causing snow to liquid equivalent ratios to be relatively higher. It is clear that the vertical temperature and moisture profiles support relatively low snow to liquid equiva-

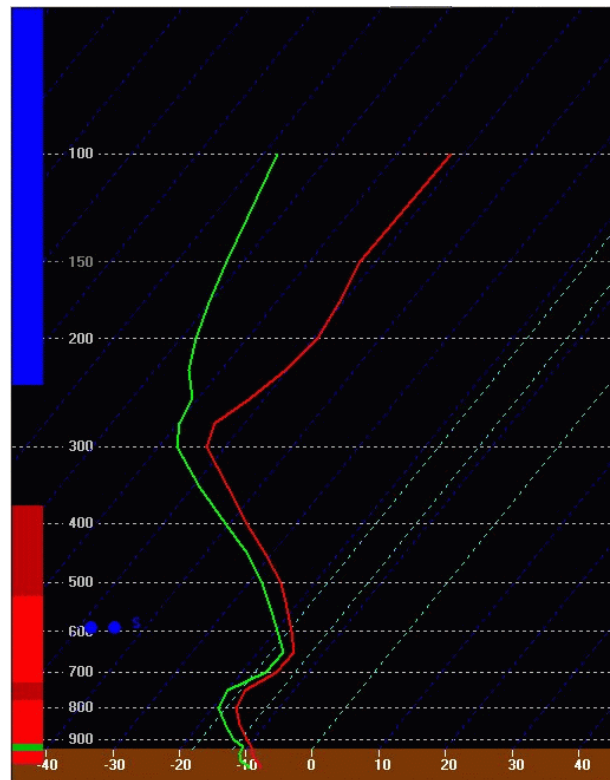


Figure 14: As in Fig. 13, but at station PHP for 0000 UTC 27 November 2001.

lent ratios in the vicinity of ILL (8-12 to 1 as shown in Fig. 9), and relatively high snow to liquid equivalent ratios in the vicinity of PHP (20-24 to 1 as shown in Fig. 9).

5. CONCLUDING REMARKS

A conceptual model detailing the processes associated with heavy banded snowfall in the presence of an ETC has been presented. The case study supports the conceptual model in its alignment of the trowal airstream, mid-level frontogenesis, and reduction of EPV. These processes act synergistically to focus vertical motion, deep layer moisture, and instability over a mesoscale zone. This work has presented the conceptual model for a given time period, future work should involve an investigation of the evolution of these processes.

The processes associated with heavy banded snowfall can be used to determine a liquid equivalent forecast (QPF), but a snow to liquid equivalent ratio must be utilized to determine a snowfall amount. A 30-year climatology of snow to liquid equivalent ratio was presented. The snow to liquid equivalent ratios for the 12 h period ending 27 November 2001 exhibited considerable stratification, elucidating the factors that determine snow to liquid equivalent ratio. The vertical profiles of temperature and moisture were analyzed, providing the type of ice crystals that likely formed. In the case presented, the climatological value of snow to liquid equivalent ratio can be used as a “first guess”. It is hoped that some skill in forecasting (relative to climatology) can be attained based upon analysis of the vertical profile of temperature and moisture as well as the surface conditions.

6. ACKNOWLEDGEMENTS

Primary funding for this research is from the Collaborative Science, Technology, and Applied Research (CSTAR) Program of NOAA under award number NA03-NWS4680019.

*

REFERENCES

- Auer, A., and J. White, 1980: The combined role of kinematics, thermodynamics and cloud physics associated with heavy snowfall episodes. *Journ. Met. Soc. Jap.*, **60**, 500–507.
- Bellamy, J., 1949: Objective calculations of divergence, vertical velocity, and vorticity. *Bull. Amer. Meteor. Soc.*, **30**, 45–49.
- Carlson, T., 1980: Airflow through midlatitude cyclones and the comma cloud pattern. *Mon. Wea. Rev.*, **108**, 1498–1509.
- Crocker, A. M., W. L. Godson, and C. M. Penner, 1947: Frontal contour charts. *J. Meteor.*, **4**, 95–99.
- Godson, W. L., 1951: Synoptic properties of frontal surfaces. *Quart. J. R. Meteor. Soc.*, **77**, 633–653.
- Holton, J., 1992: *An Introduction to Dynamic Meteorology*. Academic Press, 3rd ed., 511 pp.
- Magono, C., and C. Lee, 1966: Meteorological classification of natural snow crystals. *J. Fac. Sci., Hokkaido University*, **II**, 321–335.
- Martin, J. E., 1998a: The structure and evolution of a continental winter cyclone. Part I: Frontal structure and the occlusion process. *Mon. Wea. Rev.*, **126**, 303–328.
- , 1998b: The structure and evolution of a continental winter cyclone. Part II: Frontal forcing of an extreme snow event. *Mon. Wea. Rev.*, **126**, 329–348.
- , 1999: Quasigeostrophic forcing of ascent in the occluded sector of cyclones and the trowal airstream. *Mon. Wea. Rev.*, **127**, 70–88.
- McCann, D., 1995: Three-dimensional computations of equivalent potential vorticity. *Wea. Forecasting*, **10**, 798–802.
- Miller, J., 1948: On the concept of frontogenesis. *J. Meteor.*, **5**, 169–171.
- Nicosia, D., and R. Grumm, 1999: Mesoscale band formation in three major northeastern United States snowstorms. *Wea. Forecasting*, **12**, 346–368.
- Schultz, D. M., 2001: Reexamining the cold conveyor belt. *Mon. Wea. Rev.*, **129**, 2205–2225.
- Smith, J., 2003: *Examining the spectrum of large-scale forcing of weak, moderate, and strong cyclogenesis associated with heavy snowfall*. Master’s thesis, Saint Louis University, Department of Earth and Atmospheric Sciences, 107 pp.
- Waldstreicher, J., 2001: The importance of snow microphysics for large snowfalls. <http://www.erh.noaa.gov/er/hq/ssd/snowmicro/>.